

Numerical simulation of beam-shaped soil structure reinforced by geosynthetics

Hideki Ohta, Sami Goren, Atsushi Iizuka & Takayuki Yamakami
 Kanazawa University, Japan

Katsuaki Yamagishi
 Obayashi Co., Japan

Nobuchika Moroto
 Hachinohe Institute of Technology, Japan

ABSTRACT: A full-scale model test was conducted to investigate the mechanism of soil reinforcement by geosynthetic materials. A beam shaped soil structure reinforced by geosynthetics was designed and the global momentum stiffness was examined. This paper presents a brief description of the theoretical estimate of the global momentum stiffness of the reinforced structure for the laboratory model test and the numerical simulation of the full scale model test. The numerical simulation and the field test indicate that the effect of soil confinement by the geosynthetic material was particularly significant. A comparison of the numerical and field results is also presented.

1. INTRODUCTION

This paper presents the laboratory model test, the full scale in-situ test which are carried out to examine the global stiffness of the soils reinforced by geosynthetics against the bending moment, and a series of two dimensional finite element simulations. The laboratory test was aimed at providing basic data on the momentum stiffness of soils reinforced by geosynthetics to the design of the full scale in-situ test. The technique of numerical simulation considering the effect of confining pressure on the stress and strain soil behavior is developed and the applicability of it to the soils reinforced by geosynthetics is examined.

2. LABORATORY MODEL TEST

The momentum stiffness of the layered-reinforced sandy structure was measured using the laboratory test equipment shown in Fig.1. The container used as the equipment was 30 cm high, 50 cm wide and 84cm deep. The rectangular lumbers, 4 x 4 cm, were placed at

the bottom as the support (a) and the deformations of the reinforced soil structure (c) were measured by the dial gauges (e) as sand was removed from area (b) between 4 x 4 cm lumbers. The soil consists of dry Toyoura sand ($\rho_t=1.37\text{g/cm}^3$). Toilet paper was chosen as the reinforcement material and the stress and strain relation obtained from the uni-extension test is shown in Fig.2.

In the experiment, the number of layers of reinforcement materials (toilet paper) laid in the sand (1 up to 28 layers), the span of the structure (the width of the portion (b), 16 up to 24cm) and the height of the structure (4.9 to 13.1cm) were changed. Thus, by means of measuring the deformation of the beam-shaped structure, the global momentum stiffness, EI , of the structure was estimated based on the linearly-elastic beam theory: $EI=qL^4/(384Y_{max})$,

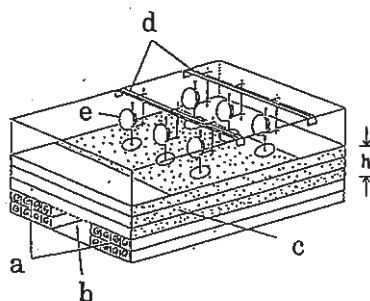


Fig.1 Laboratory model test apparatus

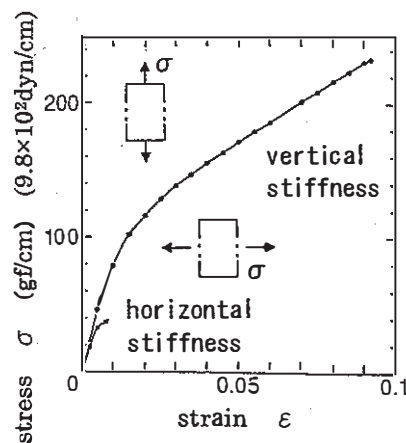


Fig.2 Stress and strain relation of toilet paper

where Y_{max} is the measured deformation, q is the load applying to the structure; $q=1.37h$ gf/cm^2 , h is the height of the structure and L is the span. Now, let us look at the influence of the span, the height of the structure and the number of laid reinforcement materials on the global momentum stiffness. Fig.3 shows the relation of Y_{max}/L and h/L , in which the measured values are plotted with the theoretical predictions indicated by the solid and broken lines. In Fig.4, the equivalent Young's modulus, E , estimated from the global momentum stiffness is plotted against the number of reinforcement materials, n , laid in the sand per a unit height of the structure. The results in Fig.4 indicate that the reinforcement contributes an increase of the equivalent Young's modulus but there seems to be a limiting value of Young's modulus.

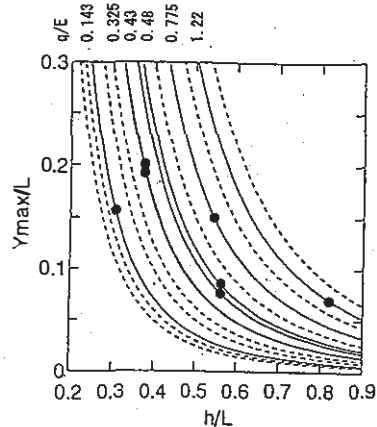


Fig.3 h/L and Y_{max}/L relation

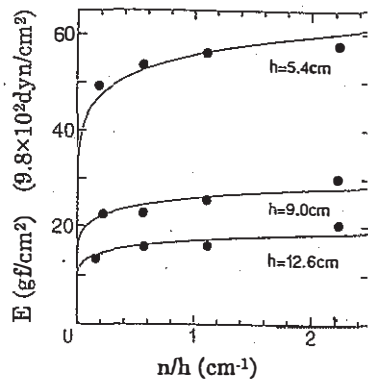


Fig.4 Geosynthetic layers and Young modulus

In order to explain the above experimental results, we introduce the following general expression,

$$E = f(E_g, E_s, n/h) \quad (1)$$

in which E is the global Young's modulus of the composite structure, E_g and E_s are Young's moduli of geosynthetics and soil respectively, n is the number of geosynthetics laid in the soil,

h is the height of the structure. If effects of E_g and E_s can be combined into a parameter, A , Eq.(1) is written as,

$$E = f(A, n/h) \quad (2)$$

In the case of the present experiment, then, by applying Eq.(2) to the curves in Fig.4, the following expression is obtained,

$$E = \{A \cdot (n/h)\}^{0.1} \quad (3)$$

in which the parameter, A has the relation with the height of the structure as indicated by plots in Fig.5. If this relation can be described by the equation: $\log(A) = a_0 + a_1 \cdot \log(h)$ as shown by the solid line in the figure, Eq.(3) becomes,

$$E = \alpha \cdot h^\beta \cdot (n/h)^m \quad (4)$$

in which α , β and m are constants. Arranging results obtained from experiment based on Eq.(4), therefore, the effect of the height of structure and the number of geosynthetics laid in the sand on the global Young's modulus is quantitatively explained as shown in Fig.6, where in the present experiment $\alpha = 2.33 \times 10^6$ ($gf/cm^2 \cdot cm^{m-\beta}$) and $\beta = -1.4$, $m = 1.0$.

However, we should note here that, Eq.(4) is an empirical equation that only applies to some special cases such as the beam-shaped reinforced structure being discussed here.

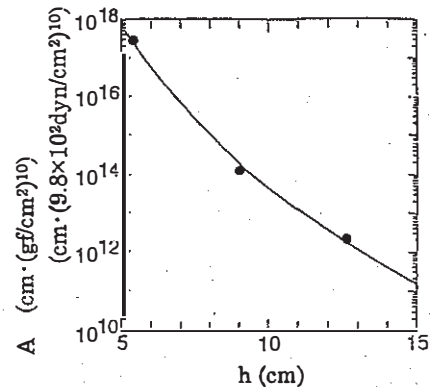


Fig.5 h and A relation

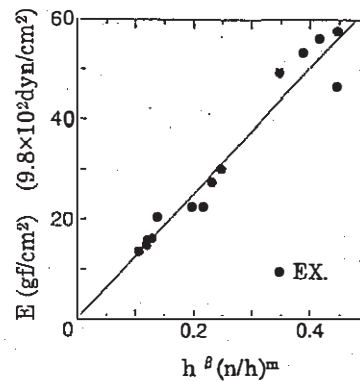


Fig.6 Dependency of n and h

3. F.E.SIMULATION OF LABORATORY TEST

The two dimensional finite element program, DACSAR (Iizuka and Ohta, 1987), was used to simulate the laboratory experiment. The program was modified to incorporate non-linear elastic constitutive relations as shown in Figs.7 and 8 to model the soil and the geosynthetics respectively (e.g., Duncan and Chang, 1970). The model for the soil (Fig.7) is described as,

$$\frac{q}{p_0} = \frac{\varepsilon_a}{a + b\varepsilon_a} \quad (5)$$

in which q is the stress difference between principal stresses, p_0 is the initial mean stress, ε_a is the axial strain and a and b are material constants. The parameters a and b are determined from the triaxial CU test stress and strain data. In the two dimensional finite element programming, Eq.(5) is rewritten in terms of the generalized stress deviator, $q = \sqrt{\frac{3}{2}s_{ij}s_{ij}}$ (is the deviatoric stress component) and the generalized strain deviator, $\gamma = \sqrt{\frac{3}{2}e_{ij}e_{ij}}$ (is the deviatoric strain component) and then

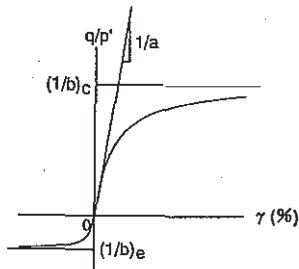


Fig.7 Stress and strain model for sand

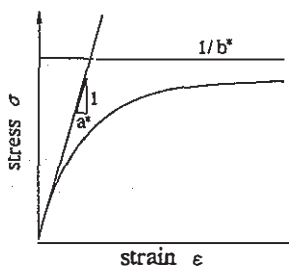


Fig.8 Stress and strain model for toilet paper

the incremental form of it is employed in the step by step calculation scheme. Therefore, the constant modulus (elastic shear modulus) between dq and $d\gamma$ is expressed as,

$$G = \frac{3ap_0}{(3a + 2b\gamma)^2} \quad (6)$$

In the present simulation, the input parameters are determined from the triaxial CU test results

for Toyoura sand reported by Fukushima and Tatsuoka, 1984 : $\alpha = 2.72 \times 10^{-3}$ and $\beta = 3.78 \times 10^{-1}$.

The non-linear elastic constitutive relation for the geosynthetic material was represented by,

$$\sigma = \frac{\varepsilon}{a^* + b^* \varepsilon} \quad (7)$$

Therefore, Young's modulus in a certain step is expressed as,

$$E = d\sigma/d\varepsilon = E_i(1 - \sigma/\sigma_{max})^2 \quad (8)$$

and $E_i = 1/a^*$, $\sigma_{max} = 1/b^*$

The input parameters needed in the computation are determined from the experimental results in Fig.2 as $E_i = 5130$ (tf/m²), $\sigma_{max} = 151$ (tf/cm²).

In the simulation, the whole composite structure was modelled by 340 4-node quadrilateral constant strain elements and the geosynthetic reinforcement was modelled by bar elements. Figs.9 shows the experimental and finite element results of the effect of reinforcement on the maximum deformation at the center of the structure and Fig.10 illustrates the predicted contribution of reinforcement to

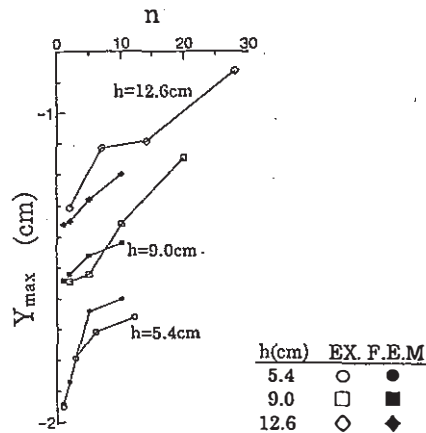


Fig.9 Y_{max} and n relation

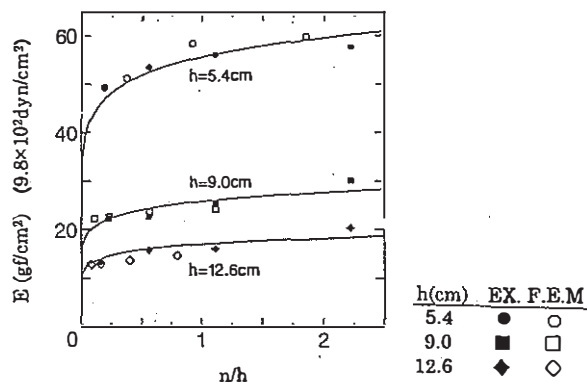


Fig.10 n/h and E relation

the elastic stiffness of the structure. The Young's modulus in Fig.10 is not directly obtained from the simulation/experiment but is estimated from the maximum deformation at the center of the structure based on the linearly elastic beam theory. The numerical simulation using non-linear elastic models can successfully explain observed results in the laboratory experiment so far.

4. FULL SCALE IN-SITU MODEL TEST

To verify the beneficial effects of the reinforcement by geosynthetics which is suggested by the laboratory experiment, a full scale model test was carried out during the period from July, 20, '92 to August, 8, '92 in Kanazawa, Japan, as a joint research project by Magara Construction Co., Maeda Cohsen Co. and the geotechnical engineering laboratory, Kanazawa University (on details, see, Nishimoto et al, 1992).

The test embankment constructed was 2.75m high, 42.5m long and 4.5m wide, including supporting berm as shown in Fig.11. The geosynthetics (Adem#G-6, Maeda Cohsen Co.) were placed at every 50cm height of the embankment and, after every placement of geosynthetics, the soil was spread over up to 10cm thickness and compacted sufficiently by the vibration roller. The degree of compaction was measured by RI (radio isotope) method and controlled. Moreover, the stiffness of the compacted soil was measured by the π test.

Markers were installed at every 25cm interval on the side of the embankment to observe horizontal and vertical deformation and strain gauges were installed on the geosynthetics laid in the compacted soil, as shown in Fig.12. The experiment began by

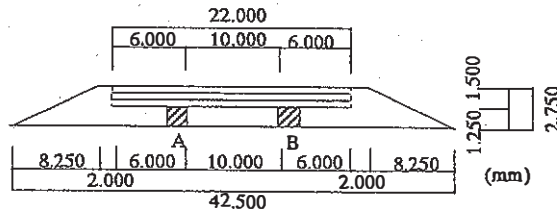


Fig.11 Side view of embankment

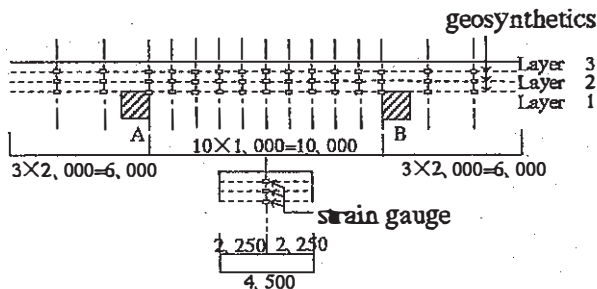


Fig.12 Location of strain gauge installed

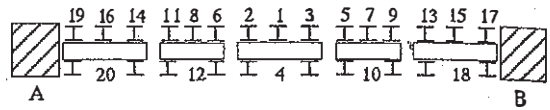


Fig.13 Position of supporting steel H piles

Table 1 Step in experiment and results

step	No. of steel pile to be removed	maximum deformation (m)
1	No.1	0.000
2	No.1~No.2	0.150
3	No.1~No.3	0.319
4	No.1~No.5	0.438
5	No.1~No.6	0.590
6	No.1~No.7	0.770
7	No.1~No.8	0.880
8	No.1~No.9	>1.200
9	No.1~No.10	>1.200

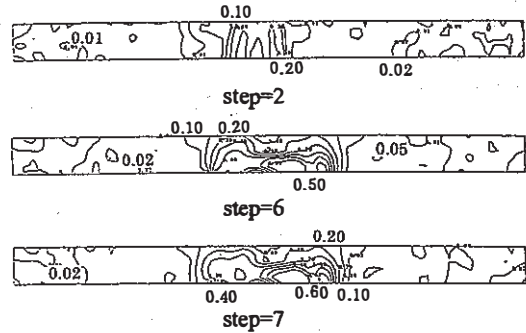


Fig.14 Contour of shear strain

removing steel H piles, which were supporting the reinforced portion by geosynthetics, in the order by the number in Fig.13.

The measured maximum deformation at each step is summarized in Table 1. Fig.14 illustrates the contours of shear strain distribution calculated from the photographic observation of the position changes of markers installed on the side of the embankment. In the experiment, when the #10 steel H pile was removed at the step 9, the structure failed.

5. F.E.SIMULATION OF IN-SITU TEST

Stress and strain characteristics of materials employed in the experiment are summarized in Figs.15 and 16. The stress and strain curves shown in Fig.15 are obtained from triaxial CU test for the soil sampled from the site. The stress and strain relation of geosynthetics (Adem #G-6) obtained from unconfined extension test is shown in Fig.16. In the numerical simulation, the soil is assumed to be a hyperbolic elastic material and the parameters needed in the model are determined from the triaxial CU test results as in Table 2 (a). The geosynthetics were modelled as linearly elastic bar elements and the parameters determined from the experiment are summarized in Table 2 (b). Since the stress and strain response of

the soil shows considerable dependency on the confining pressure, the effect of confining pressure on the soil stiffness is taken into account by employing a stress and strain model (hyperbolic model) normalized by the confining pressure. In this simulation, the initial confining pressure was computed by

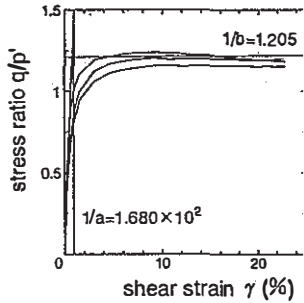


Fig. 15 Stress and strain relation of soils

Table 2 Parameters needed in analysis

(a) soil parameters			
hyperbolic			
1/a	(1/b)c	(1/b)e	γ_t (tf/m ²)
1.68×10^2	1.205	0.001	1.71

(b) geosynthetic parameters			
strength	N_t (tf/m)	6.0	
area	A (m ²)	5.25×10^{-4}	
Young modulus	E (tf/m ²)	2.60×10^5	

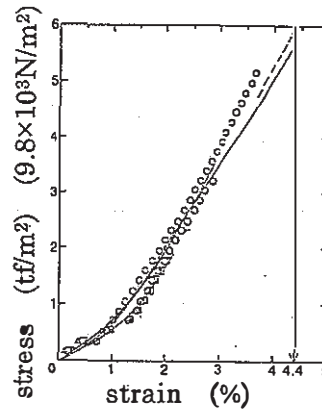


Fig. 16 Stress and strain relation of geosynthetics

applying the unit weight of in-situ soil, 1.71 tf/m³, to the structure as a body force.

In Figs. 17 (a) to (f), the computed prediction and the monitored behavior are compared for each sectional location corresponding to the pile number indicated (refer to Fig. 13), in which the horizontal axis represents the removal sequence of steel H piles by the step number in Table 1. The labels G1, G2 and G3 indicate the location where the geosynthetics are placed, that is, G1 is at the upper layer of the geosynthetics, G2 is at the middle layer and G3 is at the lower layer.

As seen from figures, the monitored deformation above the location where the steel pile was removed at the earlier step is significantly larger than our prediction. This

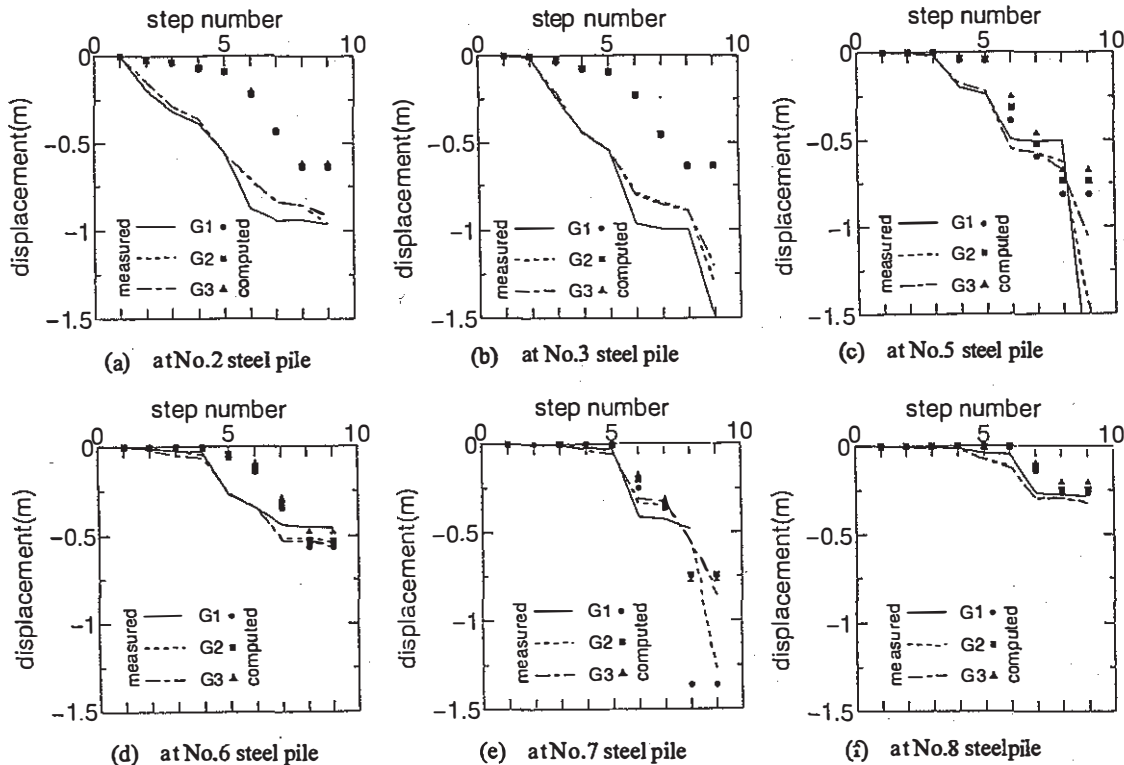


Fig. 17 Comparisons of computed deformation and monitored behavior

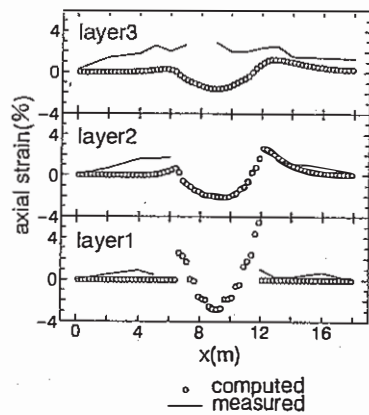


Fig.18 Axial strain of geosynthetics

would be because the geosynthetics hung down due to the removal of support so that soils between geosynthetics were loosened in the experiment. Fig.18 shows the axial strain of geosynthetics at the step of 8 (see, Table 1), in which Layer 1 indicates the upper layer, Layer 2 the middle one and Layer 3 the lower one.

6. CONCLUDING REMARKS

In this paper described are a laboratory model test, a full scale in-situ model test and a series of numerical simulation which are carried out in order to examine the momentum stiffness of the reinforced soil structure by geosynthetics. Although the geosynthetics or the soil cannot resist independently against the bending moment, their composite material shows fairly strong bending resistance. But, how strong the bending resistance is seems to depend on how well the compacted soil is wrapped by the geosynthetics. In this paper, a series of finite element simulations was carried out, where non-linear constitutive models considering the effect of confining pressure were employed. The computed results were in good agreement with the measured results in the laboratory model test but could not explain well the observed behaviors in the full scale in-situ test. It might be one reason that the geosynthetics hung down due to the removal of supporting steel piles and the soils were loosened in the experiment. But, since the soils used in the laboratory model test were very loose and the soils used in the in-situ test were well-compacted, the authors feel, at the end of this paper, that it suggests the importance of taking account of the contraction/dilatation characteristics of the soils under shearing into the numerical simulation.

REFERENCES

- Duncan, J.M. and Chang, C. (1970): Non-linear analysis of stress and strain in soils, ASCE, SM5, Vol.96, pp.1629-1653

- Fukushima, S. and Tatsuoka, F. (1984): Strength and deformation characteristics of saturated sand at extremely low pressure, *Soils and Foundations*, Vol.24, No.4, pp.30-48
- Nishimoto, T., Tsutsui, H., Morikage, A. (1992): Joint project of full scale model test for reinforced soils by geosynthetics, Research Institute Report, Magara Construction Co. (in Japanese)
- Iizuka, A. and Ohta, H. (1987): A determination procedure of input parameters in elastoviscoplastic finite element analysis, *Soils and Foundations*, Vol.27, No.3, pp.71-87